Biosketch

Keiichiro Iwao, MD, PhD, received his doctorate from Saga University's Graduate School of Medicine, Saga, Japan, in 2009, which was based on mouse models of developmental glaucoma. He is currently assistant professor in the Department of Ophthalmology, Saga University Faculty of Medicine. He has been recognized by the Association for Research in Vision and Ophthalmology and was a recipient of the 2009 Kowa Travel Grant Award. His interests include glaucoma surgery and regeneration of the optic nerve.

Jpn J Ophthalmol (2011) 55:294–300
DOI 10.1007/s10384-011-0012-8

LABORATORY INVESTIGATION

D-Allose as ischemic retina injury inhibitor during rabbit vitrectomy

Masanori Mizote · Kazuyuki Hirooka · Kouki Fukuda · Takehiro Nakamura · Toshifumi Itano · Fumio Shiraga

Received: 19 April 2010 / Accepted: 16 November 2010 / Published online: 13 May 2011

Abstract
Purpose To investigate the protective effects of D-allose, a rare sugar, on pressure-induced ischemia during vitrectomy in the rabbit eye.
Methods The rabbits underwent pars plana vitrectomy, and continuous intraocular irrigation at a perfusion pressure of 140 mmHg was performed for 45 min. Intraocular pressure was regulated by adjusting the height of a bottle of balanced saline solution containing D-allose. Morphometric studies were performed to study the effects of D-allose on the histological changes induced by ischemia in the rabbit retina. Electroretinograms (ERGs) were taken before and 1 and 7 days after vitrectomy. Nitroblue tetrazolium was used as an index of superoxide anion ($O_2^{\cdot-}$) generation. Data were analyzed by use of the unpaired Student's *t* test.
Results Seven days after ischemia, significant reductions in both number of ganglion cells and the thickness of the inner plexiform layer were observed. D-Allose significantly inhibited ischemic injury of the inner retina ($P < 0.05$). On postoperative day 7, amplitudes of ERG b-waves were significantly lower in the control group than in the D-allose group ($P < 0.05$). D-Allose suppressed the production of $O_2^{\cdot-}$.
Conclusions Intraocular irrigation with D-allose during vitrectomy may protect the retina against ischemia-induced damage.

Keywords D-Allose · Neuroprotection · Retinal ischemia · Superoxide anion · Vitrectomy

Introduction

Rare sugars are monosaccharides that exist in nature in limited quantities only. Whereas naturally abundant monosaccharides such as D-glucose and D-fructose are few in number, more than 50 kinds of rare sugars have been identified. D-Allose is a rare aldo-hexose sugar produced from D-psicose by enzymes from microorganisms [1]. Murata et al. [2] examined the scavenging activity of D-allose using electron spin resonance. They showed that D-allose inhibits the production of reactive oxygen species (ROS) in a dose-dependent manner. Furthermore, we recently reported that D-allose might protect neurons against retinal ischemia–reperfusion injury by reducing extracellular glutamate and attenuating oxidative stress [3].

Improvements in the techniques of pars plana vitrectomy (PPV) have resulted in better prognosis for vision-threatening eye diseases such as macular hole, epiretinal membrane, retinal detachment, and proliferative diabetic retinopathy (PDR). However, optic nerve atrophy after successful PPV for diabetic retinopathy is one of the most serious complications and can lead to blindness [4]. Because the extent of autoregulation in the retina and optic nerve head is limited, high infusion pressures during

M. Mizote (✉)
Department of Ophthalmology, Kagawa Prefectural Central Hospital, 5-4-16 Ban, Takamatu, Kagawa 760-8557, Japan
e-mail: m-mizote@chp-kagawa.jp

K. Hirooka · K. Fukuda · F. Shiraga
Department of Ophthalmology,
Kagawa University Faculty of Medicine,
1750-1 Ikenobe, Miki, Kagawa 761-0793, Japan

T. Nakamura · T. Itano
Department of Neurobiology,
Kagawa University Faculty of Medicine,
1750-1 Ikenobe, Miki, Kagawa 761-0793, Japan

vitreous surgery may cause retinal ischemia and lead to damage of the retina and optic nerve.

During or after ischemia, ROS such as hydrogen peroxide (H_2O_2), superoxide anion (O_2^-) and hydroxyl radical (OH^-) can be produced in large quantities and act as cytotoxic metabolites. ROS have been implicated in the process of apoptosis, because treatment of cells with ROS can result in this form of cell death, whereas application of antioxidants can prevent it under some conditions [5, 6]. ROS scavengers have been shown to be neuroprotective against ischemia in acute experimental models [7].

The purpose of this study was to investigate the protective effects of D-allose on pressure-induced ischemia during vitrectomy in the rabbit eye.

Materials and methods

Animals

Female New Zealand White rabbits, weighing 2.0–2.4 kg, were obtained from Kitayama Labs KK (Nagano, Japan). The rabbits were anesthetized by intraperitoneal injection of ketamine (50 mg/kg) and xylazine (10 mg/kg). Animal care and experiments followed the standard guidelines for animal experimentation of Kagawa University Faculty of Medicine and adhered to the ARVO Statement for the Use of Animals in Ophthalmic and Vision Research. The animals were divided into two groups according to the intraocular irrigating solutions they received: the vehicle group, using a balanced saline solution (BSS) alone, and the D-allose group, using BSS + D-allose (2%).

Vitrectomy and subsequent vitreous perfusion

A 250-ml bottle of intraocular irrigating solution (BSS; Alcon Laboratories, Fort Worth, TX, USA) was suspended approximately 100 cm above the eye level of each rabbit, and connected to a 20-gauge infusion cannula through a 200-cm-long tube. The infusion cannula was inserted through the sclerotomy in the inferonasal quadrant 3 mm posterior to the limbus, and sutured in place. A vitreous cutter (MVS XX; Alcon) was placed through the sclerotomy in the supratemporal quadrant, and vitrectomy was then performed for 10 min. The vitreous cavity was irrigated during vitrectomy either with BSS alone or with BSS + D-allose. Adequate illumination was provided by a paraxial light operation microscope without intraocular fiberoptic illumination. If retinal tear or retinal detachment occurred during vitrectomy, those animals were excluded from the experiment. After completion of the vitrectomy, the cutter was removed and the sclerotomy wound was tightly sutured using a 7-0 vicryl. Intraocular pressure (IOP) was raised to 140 mmHg for 45 m by elevating the solution bottle. Retinal ischemia was confirmed by whitening of the fundus. Rectal temperature was monitored throughout the surgery. Because body temperature during vitrectomy in acute ischemic eyes may affect ischemia-induced retinal damage [8, 9], rectal and tympanic temperature was maintained at approximately 37°C by use of a feedback-controlled heating pad (BRC, Nagoya, Japan) during the operation. After restoration of blood flow, the temperature was continuously maintained at 37°C. Eyes were treated topically with levofloxacin (Santen Pharmaceutical, Osaka, Japan) after surgery to prevent postoperative infection.

Electroretinograms (ERGs)

Before surgery, ERG responses were measured after 20 min of dark adaptation using a recording device (Mayo, Aichi, Japan). The procedure was repeated on postoperative days 1 and 7. ERGs were recorded by positioning the rabbit in a box and placing a xenon lamp 15 cm in front of the eye. A flash of maximum intensity 20 J provided photostimulation. A contact lens electrode was placed on the cornea, and a reference electrode subcutaneously at the vertex. ERGs were taken of both eyes for each animal. The a- and b-wave amplitudes of each operated eye were shown as a percentage of those in the pre-operated eye.

Histological examination

For histological examination, the rabbits were anesthetized by intraperitoneal injection of ketamine and xylazine 1 week after ischemia and perfused intracardially with phosphate-buffered saline (PBS), followed by perfusion with 4% paraformaldehyde in PBS. Eyes were removed and embedded in paraffin, and thin sections (5-μm thickness) were cut using a microtome. Each eye was mounted on a silane-coated glass slide and then stained with hematoxylin and eosin (HE).

Morphometric analysis was performed to quantify ischemic injury. The sections for analysis were selected randomly for each eye. A microscopic image of each section within 0.5–1 mm of the optic disc was scanned. In each computer image, the thickness of the inner plexiform layer (IPL) and inner nuclear layer (INL) at the tire frame were measured. Finally, in each eye, the thicknesses of the IPL and INL were obtained as the mean values of five measurements. For each animal, these values for the right eye were normalized to those for the intact left eye and shown as a percentage.

Retrograde labeling of retinal ganglion cells (RGCs)

Seven days before the rabbits were killed, the optic nerves were exposed by lateral orbitotomy. Using a Hamilton syringe, 10 μl of a 0.1% fluorescent dye (Fast Blue; Polysciences, Warrington, PA, USA) was injected into the optic nerve 2 mm behind the eyeball. Care was taken not to injure any blood vessels, especially the ophthalmic artery that enters the sclera from the ventral margin of the optic nerve. After the surgery the eyes were treated topically with levofloxacin.

Assessment of RGC survival

Animals were killed by an overdose of ketamine and xylazine 1 week after the fast blue application. Whole, flat-mounted retinas were then assayed for the retinal ganglion cell density. The rabbit eyes were enucleated and fixed in 4% paraformaldehyde for 10 h at room temperature. After removal of the anterior segments, the resulting posterior eyecups were left in place. Subsequently, 4 radial cuts were made in the periphery of each eyecup, with the retina then carefully separated from the retinal pigment epithelium. To prepare the flat mounts, the retina was dissociated from the underlying structures, flattened by making 4 radial cuts, and then spread on a gelatin-coated glass slide. Labeled RGCs were visualized under a fluorescence microscope (Olympus BX-51/DP70; Olympus, Tokyo, Japan) by using a filter set (excitation filter 330–385 nm; barrier filter 420 nm; WU; Olympus). Fluorescence-labeled RGCs were counted in 12 microscopic fields of retinal tissue from 2 regions in each quadrant at 2 different eccentricities, central and peripheral. We counted the RGCs in each eye by using Image-Pro Plus software (Version 4.0; Media Cybernetics, The Imaging Expert, Bethesda, MD, USA). Cell counts were conducted by the same person in a masked fashion, with the identity of the original retinas unknown to the investigator until all cell counts from all the different groups were completed. Changes in the densities of the RGCs were expressed as the RGC survival percentage, which was based on comparison of the surgical and contralateral control eyes. The specimens that were compared came from different retinal regions of the same animal.

O_2^- analysis

O_2^- generation was determined by measuring the reduction of nitroblue tetrazolium (NBT) to a diformazan precipitate as previously described [10]. NBT (50 mg/ml; Research Organics, Cleveland, OH, USA) was dissolved in dimethylformamide (DMF) and distilled BSS. The final DMF concentration was 10%. Reduction was detected by intravitreal injection of 5-μl NBT solution in the period after vitrectomy before ischemia. For observation of the diformazan precipitate, a microscope (S5; Carl Zeiss, München, Germany) was used with a 3CCD digital camera (MKC-507; Ikegami Tsushinki, Tokyo, Japan) and recorded using a DVD recorder.

Statistical analysis

Image analysis was performed with Image-Pro Plus software (The Imaging Expert) to assess O_2^- generation area density. We determined the total blue-stained area indicated O_2^- generation area. Evaluation by Image-Pro Plus analysis of photographs was performed blind by two researchers not directly involved in this study and the generation area was automatically produced by the software. All statistical values are presented as mean ± standard deviation (SD). Data were analyzed by use of the unpaired Student's t test. Values of $p < 0.05$ were considered statistically significant.

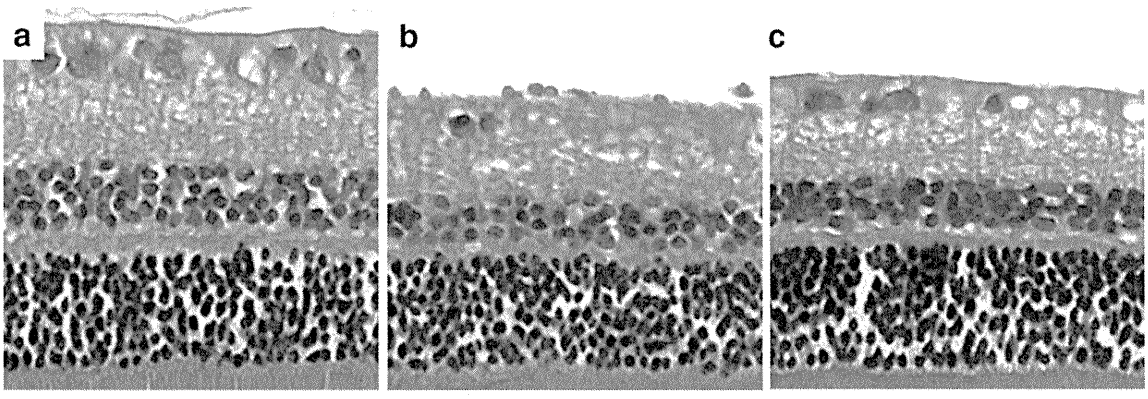

Fig. 1 Light micrographs of a cross-section of **a** hematoxylin and eosin histology through normal rabbit retina and **b** 7 days after ischemia with balanced salt solution (BSS) alone, or **c** BSS + D-allose. Cell loss in the ganglion cell layer (GCL) and reduced inner nuclear layer (INL) thickness were ameliorated in the D-allose group. *Bar* 10 μm

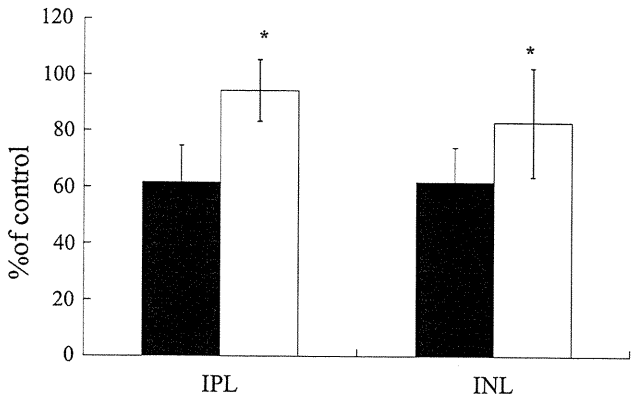

Fig. 2 Percentage changes relative to control values in the thicknesses of the IPL and INL 7 days after ischemia with BSS alone and BSS + D-allose. *Black bar* D-allose group, *white bar* vehicle group. Administration of 2% D-allose significantly prevented the reduction in the number of cells in the GCL and the thickness of the INL. Results are expressed as mean ± standard deviation (SD). $*P < 0.05$

Results

Histological change in the retina after ischemia with and without D-allose

Figure 1a shows a normal retina. Light-microscopic photographs were taken 7 days after ischemia (Fig. 1b, c). The retina of the untreated eye in the animals, was used as control. In the vehicle group, significant reductions in the thickness of the INL were observed. The thickness of the IPL was 61.6 ± 13.0% that of the control and the thickness of the INL was reduced to 61.8 ± 12.2% that of the control ($n = 6$; Fig. 2). In the D-allose group, the thickness of the IPL was 94.2 ± 11.1% that of the control and the thickness of the INL was 82.9 ± 19.4% that of the control ($n = 5$; Fig. 2). Reduced INL thickness was ameliorated in the D-allose group.

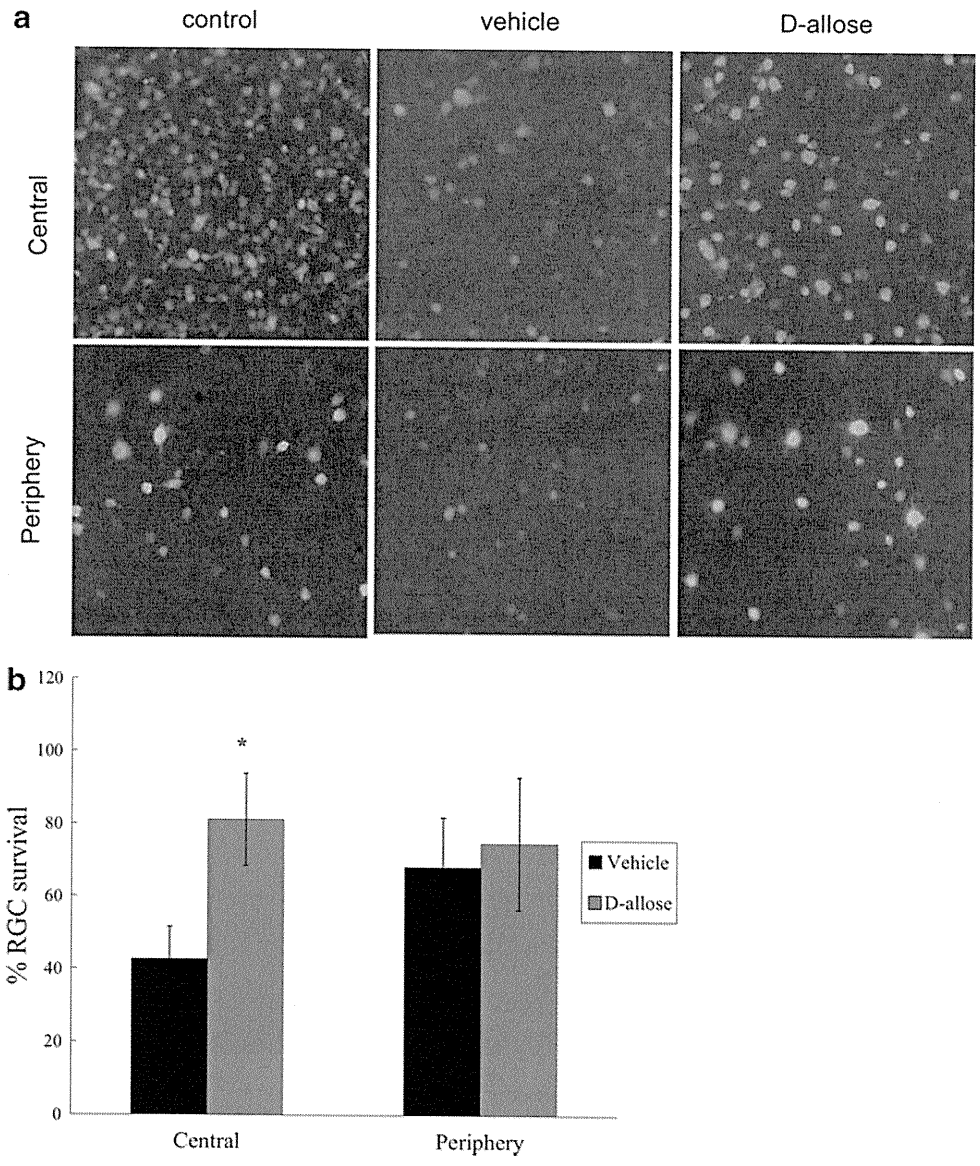

Fig. 3 Effects of D-allose on ischemia-induced retinal ganglion cell (RGC) death. **a** Retrograde labeling of RGCs in nonischemic eyes, and **b** 7 days after ischemic injury treated with vehicle or D-allose. *Bar* 100 μm. RGCs were counted in the central and peripheral areas. *Gray bar* D-allose group, *black bar* vehicle group. Graph depicts the mean ± SD for three rabbits treated with vehicle and three rabbits treated with D-allose. $*P < 0.05$

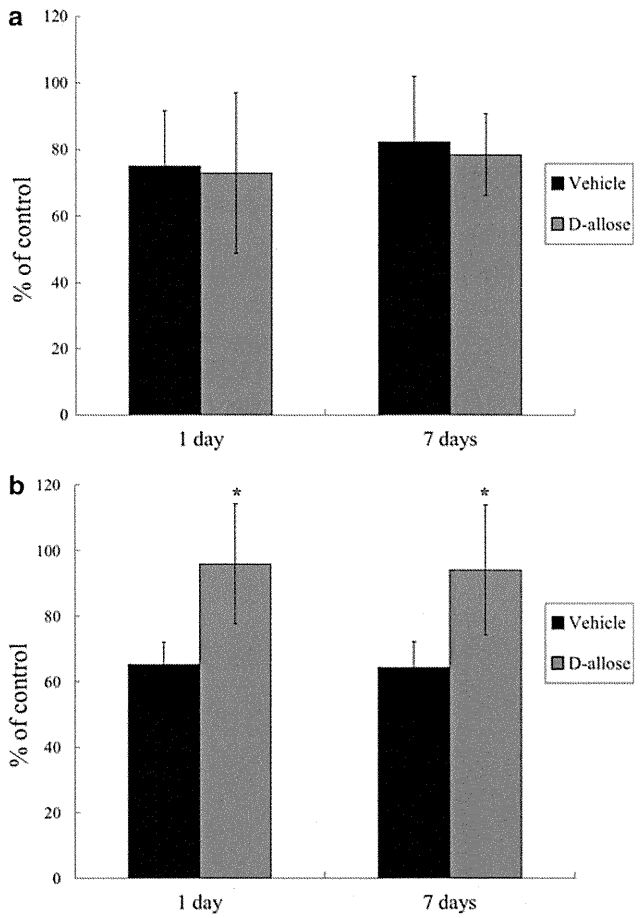

Fig. 4 **a** On postoperative day 7, the a-wave amplitude was 78.4 ± 12.3% in the D-allose group and 82.3 ± 19.6% in the vehicle group. *Gray bar* D-allose group, *black bar* vehicle group. **b** The b-wave amplitudes were 94.1 ± 19.8 and 64.3 ± 7.9%, respectively. On postoperative days 1 and 7, the mean amplitude of the b-wave for eyes treated with D-allose was significantly higher than for those treated with vehicle. *Gray bar* D-allose group, *black bar* vehicle group. Results are expressed as mean ± SD. *$P < 0.05$

Survival of RGCs

Figure 3a shows representative results of RGC labeling for both vehicle and D-allose-treated rabbits. RGC survival in the central retinas of the eyes with ischemia was 42.8 ± 8.8% in the vehicle-treated group ($n = 4$) and 81.2 ± 12.7% in the D-allose-treated group ($n = 4$, $P = 0.01$; Fig. 3b). In the peripheral retina, RGC survival in eyes with ischemia was 68.0 ± 13.8% in the vehicle-treated group and 74.7 ± 18.3% in the D-allose-treated group ($P = 0.64$; Fig. 3b).

ERGs

The mean amplitudes of both the a-wave and b-wave are shown in Fig. 4. On postoperative day 7, the a-wave amplitude was 78.4 ± 12.3% in the D-allose group ($n = 5$) and 82.3 ± 19.6% in the vehicle group ($n = 5$; Fig. 4a). The b-wave amplitudes were 94.1 ± 19.8 and 64.3 ± 7.9%, respectively (Fig. 4b). The mean amplitude of the b-wave in eyes treated with D-allose was significantly higher than in those treated with vehicle. Likewise, no significant differences in the mean amplitude of a-waves were identified between the D-allose and vehicle groups. Both a-wave and b-wave amplitudes in the non-operated eyes were stable and essentially equal both before and after surgery.

Effects of D-allose on released O_2^-

Light-microscopic photographs were taken after treatment without D-allose, i.e., BSS alone (Fig. 5a), and with D-allose (Fig. 5b). Without D-allose treatment, the blue color was observed after ischemia and became stronger over time. However, in the presence of D-allose, the blue color

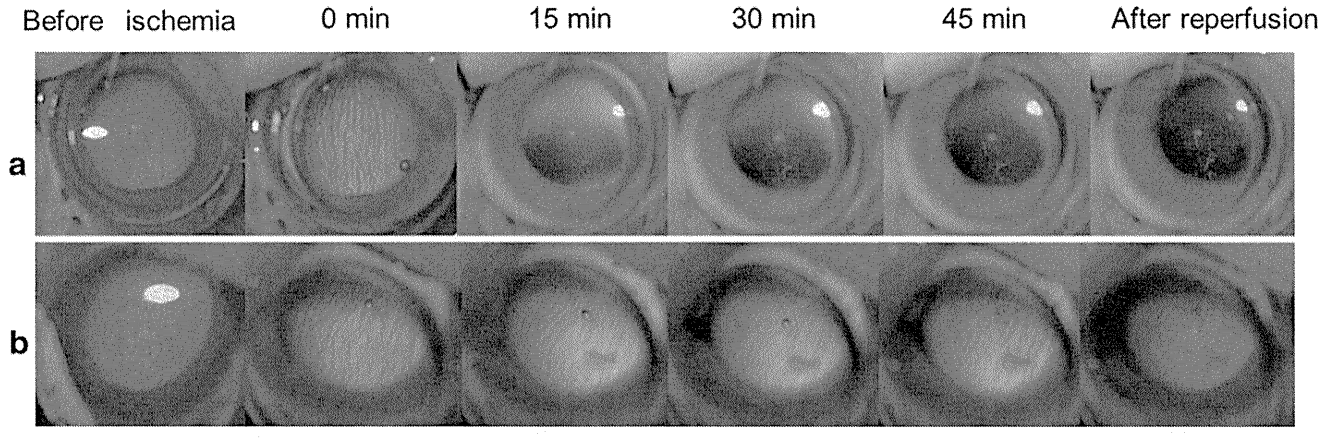

Fig. 5 Effects of D-allose on the release of superoxide anion (O_2^-). *Blue color* indicates release of O_2^-. Ischemia was induced for 45 min. Color photographs were taken before ischemia induction, then 0, 15, 30 and 45 min after starting ischemia, then immediately after reperfusion. **a** Vehicle group and **b** D-allose group

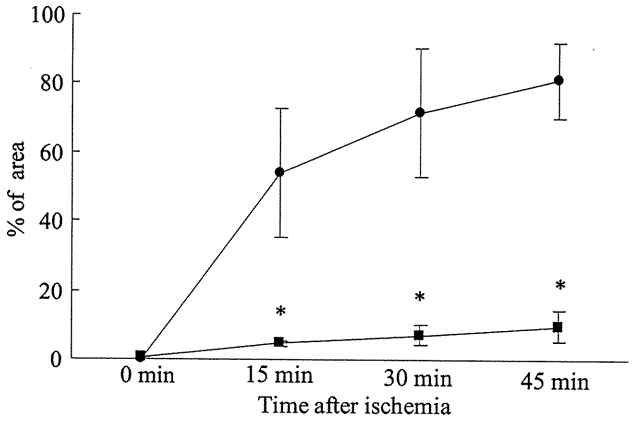

Fig. 6 Measured area O_2^- expression (%). *Filled squares* D-Allose group, *filled circles* vehicle group. Comparison of mean values of O_2^- expression between the vehicle group and the D-allose group at each time point. Mean O_2^- expression was significantly different 15, 30, and 45 min after ischemia. Data are mean ± SD. $*P < 0.05$

decreased compared with that without D-allose. Compared with the peripheral area, the blue color intensity was stronger in the central area. Figure 6 shows results from quantification of the color levels expressed as a percentage change. Mean O_2^- expression was significantly different between the vehicle group and the D-allose group 15, 30, and 45 min after ischemia.

Discussion

These findings show that intraocular irrigation with D-allose during vitrectomy protects the morphology and function of the retina against ischemia injury.

Because D-allose may inhibit hexose transport [11], co-injection of 200 mg/kg glucose with 200 mg/kg D-allose has been shown to have no protective effect against retinal ischemia reperfusion injury [3]. BSS contains 5.11 mM glucose; i.e., approximately 0.1% glucose. Because 2% D-allose in BSS was used in this study, the glucose in BSS was not sufficient to abolish the protective effects of D-allose.

Both clinically and under experimental conditions, the functional status of the retina can be monitored continuously by recording ERGs. The b-wave of the ERG has been identified as a particularly sensitive index of retinal ischemia both in humans [12] and in experimental models of retinal ischemia in vitro [13]. Glutamate acts as a mediator of neuronal injury under ischemic conditions [14] and extracellular glutamate has been found to increase in ischemic eyes [3, 15, 16]. Reperfusion injury is thought to be mediated in part by relative hyperglycemia and high oxygen levels, leading to oxygen radical formation. D-Allose may be a down-regulation agent of hexose transport [11]. D-Allose could reduce the production of ROS by modulating the glycolytic response. Because D-allose can suppress glutamate release and the production of ROS after ischemia [3], D-allose protects both the morphology and function of the retina. Because there were no morphological changes in the outer retina in this study (data not shown), recovery of the a-wave amplitudes in the vehicle group was not suppressed. Therefore, we could not confirm any differences in the recovery of a-wave amplitudes between the vehicle and D-allose groups.

We recently reported that D-allose suppresses the production of H_2O_2 as determined by diaminobenzidine solution without hydrogen peroxide [3]. NBT is an electron acceptor that can be reduced by accepting electrons from various reductants, including superoxide [17] and other reductants, for example those generated from dehydrogenase systems [18, 19]. Studies have previously shown that NBT staining in normal rat retina is affected by inhibition of free radical-related enzyme systems, suggesting that NBT might be useful in the study of free radicals. During and after ischemic episodes, univalent reduction of oxygen in the mitochondrial respiratory chain is thought to be a major source of O_2^- [20]. O_2^- can be reduced to H_2O_2, a reaction catalyzed by superoxide dismutase (SOD) [7]. H_2O_2 has been identified as a potent inducer of apoptosis [21]. D-Allose may exert neuroprotective effects by reducing the production of not only H_2O_2, but also O_2^-.

Ocular perfusion pressure would be especially important in eyes with diabetes if, as has been suggested, autoregulation in the retina and optic nerve head is impaired [22, 23]. Because high infusion pressure during PPV is useful in preventing bleeding, we must also consider protecting the retina against damage caused by pressure-induced ischemia in cases of diabetic retinopathy [24]. Levels of glutamate potentially toxic to retinal ganglion cells have been found in the vitreous of patients with PDR [25]. This glutamate could then initiate a forward cascade of further neuronal ischemia.

Our findings suggest that intraocular irrigation with D-allose during vitrectomy may protect both the morphology and function of the retina against ischemia-induced damage.

Acknowledgments This work was supported by a Grant-in-Aid for Scientific Research from the Ministry of Education, Culture, Sports, Science, and Technology of Japan (20592078).

References

1. Bhuiyan SH, Itami Y, Yuhko R, Katayama T, Izumori K. D-Allose production from D-psicose using immobilized L-rhamnose isomerase. J Ferment Bioeng. 1998;85:540–2.
2. Murata A, Sekiya K, Watanabe Y, Yamaguchi F, Hatano N, Izumori K, et al. A novel inhibitory effect of D-allose on production of reactive oxygen species from neutrophils. J Biosci Bioeng. 2003;96:89–91.
3. Hirooka K, Miyamoto O, Jinming P, Du Y, Itano T, Baba T, et al. Neuroprotective effect of D-allose against retinal ischemia–reperfusion injury. Invest Ophthalmol Vis Sci. 2006;47:1653–7.

4. Seki M, Togashi H, Ando N. Optic nerve atrophy after vitrectomy for diabetic retinopathy: its systemic and local risk factors. Nippon Ganka Gakkai Zasshi. 2006;110:462–7.
5. Jacobson MD. Reactive oxygen species and programmed cell death. Trends Biochem Sci. 1996;21:83–6.
6. Kroemer G, Petit P, Zamzami N, Vayssière JL, Mignotte B. The biochemistry of programmed cell death. FASEB J. 1995;9:1277–87.
7. Bonne C, Muller A, Villain M. Free radicals in retinal ischemia. Gen Pharmacol. 1998;30:275–80.
8. Tamai K, Toumoto E, Majima A. Local hypothermia protects the retina from ischemic injury in vitrectomy. Br J Ophthalmol. 1997;81:789–94.
9. Traustason S, Eysteinsson T, Agnarsson BA, Stefánsson E. GABA agonists fail to protect the retina from ischemia–reperfusion injury. Exp Eye Res. 2009;88:361–6.
10. Digregorio KA, Cilento EV, Lantz RC. Measurement of superoxide release from single pulmonary alveolar macrophages. Am J Physiol. 1987;252:C677–83.
11. Ullrey DB, Kalckar HM. Search for cellular phosphorylation products of D-allose. Proc Natl Acad Sci USA. 1991;88:1504–5.
12. Coleman K, Fitzgerald D, Eustace, Bouchier-Hayes D, et al. Electroretinography, retinal ischemia and carotid artery disease. Eur J Vasc Surg. 1990;4:569–73.
13. Zager E, Ames A. Reduction of cellular energy requirements: screening for agents that may protect against CNS ischemia. J Neurosurg. 1988;69:568–79.
14. Choi DW. Glutamate neurotoxicity and diseases of the nervous system. Neuron. 1988;1:623–34.
15. Louzada-Junior P, Dias JJ, Santos WF, Lachat JJ, Bradford HF, Coutinho-Netto J. Glutamate release in experimental ischaemia of the retina: an approach using microdialysis. J Neurochem. 1992;59:358–63.
16. Adachi K, Kashii S, Masai H, Ueda M, Morizane C, Kaneda, et al. Mechanism of the pathogenesis of glutamate neurotoxicity in retinal ischemia. Graefes Arch Clin Exp Ophthalmol. 1998;236:766–74.
17. Auclair C, Voisin E. Nitroblue tetrazolium reduction. In: Greenwald RA, editor. Handbook of methods for oxygen radicals research. Boca Raton: CRC Press; 1988. p. 123–32.
18. Altman FP. Tetrazolium salts and formazans. Prog Histochem Cytochem. 1976;9:1–56.
19. Zhang H, Agardh E, Agardh CD. Nitro blue tetrazolium staining: a morphological demonstration of superoxide in the rat retina. Graefes Arch Ophthalmol. 1993;231:178–83.
20. Gonzalez-Flecha B, Boveris A. Mitochondrial sites of hydrogen peroxide production in reperfused rat kidney cortex. Biochim Biophys Acta. 1995;1243:361–6.
21. Hockenbery DM, Oltvai Z, Yin XM, Milliman CL, Korsmeyer SJ. Bcl-2 functions in an antioxidant pathway to prevent apoptosis. Cell. 1993;75:241–51.
22. Kohner EM, Patel V, Rassam SM. Role of blood flow and impaired autoregulation in the pathogenesis of diabetic retinopathy. Diabetes. 1995;44:603–6.
23. Arnold AC. Pathogenesis of nonarteritic anterior ischemic optic neuropathy. J Neuroophthalmol. 2003;23:157–63.
24. Ikushima M, Tano Y, Ikeda T, Sato Y. Hyper-infusion pressure for diabetic membrane dissection. Jpn J Ophthalmol. 1990;34:393–400.
25. Ambati J, Chalam KV, Chawla DK, D'Angio CT, Guillet EG, Rose SJ, et al. Elevated γ-aminobutyric acid, glutamate, and vascular endothelial growth factor levels in the vitreous of patients with proliferative diabetic retinopathy. Arch Ophthalmol. 1997;11:1161–6.

CORRELATION OF INCREASED FUNDUS AUTOFLUORESCENCE SIGNALS AT CLOSED MACULA WITH VISUAL PROGNOSIS AFTER SUCCESSFUL MACULAR HOLE SURGERY

CHIEKO SHIRAGAMI, MD, FUMIO SHIRAGA, MD, ERI NITTA, MD, KOUKI FUKUDA, MD, HIDETAKA YAMAJI, MD

Purpose: To study the significance of the increased fundus autofluorescence (FAF) signals at closed macula with spectral-domain optical coherence tomography and visual prognosis after successful surgery in eyes with idiopathic full-thickness macular holes (MHs).

Methods: Seventy-eight eyes of 78 consecutive patients with full-thickness MHs underwent successful standard vitrectomy, with internal limiting membrane peeling and followed by 10% sulfur hexafluoride gas injection. Simultaneous FAF and optical coherence tomography images were recorded at 10 days, and 1, 3, and 6 months postoperatively, using a combined spectral-domain optical coherence tomography–fluorescein angiography device (Spectralis™/HRA Heidelberg Retina Angiograph 2). The appearance of increased FAF in the macula postoperatively and the relationship of FAF and optical coherence tomography findings to best-corrected visual acuity were examined.

Results: Stage 2, 3, and 4 MHs were present in 31, 29, and 18 eyes, respectively. The median patient age was 66 years, with a range of 54 to 79 years. In all patients, the MHs were successfully closed, and the preoperative increased FAF corresponding to MH disappeared 10 days after surgery. In 36 eyes (46.2%), however, hyperautofluorescence again appeared in the macular area 1 month postoperatively. This hyperautofluorescence was significantly associated with the recovery of the external limiting membrane lines at the fovea 1 month after surgery ($P = 0.001$, multiple logistic regression analysis). Also, this recovery of the external limiting membrane lines 1 month postoperatively was significantly associated with the recovery of photoreceptor inner and outer segment junction line 3 months postoperatively at the fovea ($P < 0.001$, Fisher exact test). Moreover, a good best-corrected visual acuity of 20/28 or better at 6 months after surgery was significantly associated with hyperautofluorescence in the macula 1 month postoperatively, the recovery of the photoreceptor inner and outer segment lines at the fovea 3 months postoperatively, and preoperative good visual acuity ($P < 0.05$, multiple logistic regression analysis).

Conclusion: In full-thickness MHs, 46.2% of our patients showed increased FAF in the macula 1 month after successful MH surgery. This hyperautofluorescence could be a sign of good visual prognosis postoperatively.

RETINA 32:281–288, 2012

The macular hole (MH) is a full-thickness defect of the retinal tissue involving the anatomical fovea. Significant controversy still exists regarding the pathogenesis, prognosis, and management of this lesion.[1] The diagnosis of idiopathic full-thickness MHs is usually made by biomicroscopic examination and optical coherence tomography (OCT). Recently, a new technique has been developed that allows in vivo imaging of the distribution of fundus autofluorescence (FAF) using a confocal laser scanning ophthalmoscope.[2–4] In a normal fundus, the distribution of FAF is diffuse, with decreased intensity at the fovea. This technique provides high–spatial resolution imaging of the distribution of FAF, which is most

likely derived from lipofuscin within the retinal pigment epithelium (RPE).[4–9] It is generally accepted that lipofuscin represents the product of degradation of the photoreceptor outer segments. Therefore, an autofluorescent spot in the macula is consistent with a loss of the foveal tissue, especially a complete full-thickness MH. Disappearance of FAF from the MH, as may occur after successful surgical repair,[3,4] suggests that the RPE is again covered by the retinal and/or glial tissue, as demonstrated also by the OCT images.

Macular FAF is attenuated by the luteal pigment, and the concentration of this pigment in the fovea is densest along the outer plexiform layer.[10] Any foveal defect that spares the photoreceptors[11] may alter the degree of foveal FAF by decreasing the amount of masking macular pigment, therefore increasing the foveal FAF. In vivo imaging of FAF can be carried out with commercially available confocal scanning laser ophthalmoscopes.[9] Although the usefulness of this technique has already been demonstrated for the diagnosis of full-thickness MH, there are few reports[11] of postoperative increased FAF in the macula after successful MH closure. In another report, it was noted that MH closure is attained by bridge formation (foveal detachment) and healing of the photoreceptor inner and outer segment junction (IS/OS) line in varying degrees, which correlated with visual outcomes.[12,13] However, there was no discussion of the correlation between the OCT images and the FAF images of the external limiting membrane (ELM) line. As visualized on electron microscopic images, the external limiting membrane is formed by junctional complexes uniting the Muller cells to the photoreceptor cell inner segments. Therefore, the aims of this study were to investigate the significance of postoperative increased FAF in the macula and to determine the relationships among FAF findings, restoration of ELM and IS/OS line on OCT images, and best-corrected visual acuity (BCVA) after successful MH surgery.

Patients and Methods

Seventy-eight eyes of 78 consecutive patients (39 women and 39 men, ranging in age from 54 to 79 [mean, 66.0] years), who underwent vitrectomy for idiopathic MHs between April 2007 and April 2009, were included in the study. Both biomicroscopy and OCT were used to classify the MH stage. Eyes with reopened MHs, MHs with retinal detachment, MHs caused by high myopia, or other macular diseases, such as age-related macular degeneration (including dry type) combined, were excluded from this study. The study was conducted in accordance with the recommendations of the Declaration of Helsinki and was approved by the institutional review board at the Kagawa University Hospital. After an explanation of the purpose of the study and the procedures to be used, a signed informed consent was obtained from all patients before surgery and examinations.

Surgical Technique

Local anesthesia was induced by retrobulbar nerve block. A 25-gauge pars plana vitrectomy with internal limiting membrane (ILM) peeling was carried out in all eyes using the Accurus vitrectomy system (Alcon Labs, Fort Worth, TX). The posterior hyaloid was separated and removed using the 25-gauge vitreous cutter. Later, all vitreous traction on the MH was removed and the peripheral vitreous subtotally shaved. When the ILM was removed, brilliant blue G[14] was used for staining in 42 eyes, and in the other 36 eyes, triamcinolone acetonide–assisted ILM peeling was carried out. The area of ILM peeling was 2–3 optic disk diameters around the fovea. Cataract surgery combined with a vitrectomy was carried out in all 78 patients aged older than 50 years. At the end of the surgery, 10% sulfur hexafluoride gas was infused into the vitreous cavity. Face-down positioning was maintained for 3 postoperative days.

Ophthalmic Examinations and Fundus Photography

All patients underwent a regular ophthalmic examination, including measurement of the BCVA and fundus examination. Color fundus photography using the Topcon TRC-50DX fundus camera (Topcon, Tokyo, Japan) was carried out using 50° field images preoperatively and postoperatively (10 days, and 1, 3, and 6 months after the surgery in all patients). The FAF and foveal OCT images were recorded to simultaneously detect the intensity of FAF, and ELM and IS/OS line recovery using the combined spectral-domain OCT–fluorescein angiography device (Spectralis™/HRA Heidelberg Retina Angiograph 2, Heidelberg Engineering GmbH, Heidelberg, Germany) at 10 days, and 1, 3, and 6 months postoperatively. Foveal images were examined in both horizontal and in vertical directions, with averages of 100 scans using the automatic averaging and eye tracking features.

From the Department of Ophthalmology, Kagawa University Faculty of Medicine, Kagawa, Japan.

The authors have no proprietary, financial, or conflicts of interest to disclose.

Reprint requests: Chieko Shiragami, MD, Department of Ophthalmology, Kagawa University Faculty of Medicine, 1750-1 Ikenobe Miki-cho, Kagawa 761-0793, Japan; e-mail: chappi@kms.ac.jp

Statistical Methods

To determine whether there was a significant association between increased FAF at the closed MH area and several factors including patient age, preoperative BCVA, MH stage, and ELM and IS/OS line recovery at the fovea on OCT images 1 month postoperatively, multiple logistic regression analysis was carried out. The BCVA was converted to logMAR (logarithm of the minimal angle of resolution) equivalents for statistical analysis. Furthermore, factors predicting good BCVA of 20/28 or better (logMAR 0.15) at 6 months after surgery were analyzed, using patient age, increased FAF at 1 month after surgery, preoperative BCVA, IS/OS line recovery at 3 months after surgery, preoperative historical duration, MH stage, and the use of ILM staining as the factors. Also, the correlation between ELM line recovery at 1 month postoperatively and IS/OS line recovery at 3 months postoperatively was examined statistically (Fisher exact test). A P value of <0.05 was considered significant. Statistical analysis was carried out using SPSS 11.5 statistical software (SPSS, Inc, Chicago, IL).

Results

A total of 78 eyes of 78 patients with unilateral MHs were prospectively studied. Stage 2, 3 (Figure 1, 3A), and 4 MHs were present in 31, 29, and 18 eyes, respectively. Six months postoperatively, the mean logMAR visual acuity improved significantly from 0.61 ± 0.62 preoperatively to 0.17 ± 0.07 ($P < 0.001$, paired t-test). The historical duration of MHs, which corresponds to the duration since becoming aware of metamorphopsia or visual disturbance to receiving the operation in each patient, was 1 month to 15 months (mean 3.4 ± 2.1 months).

In all patients, the preoperative increased FAF corresponding to MHs (Figure 2A) disappeared 10 days after successful surgical closure. However, mild increased FAF signals at the closed macular regions were seen in 36 eyes (46.2%) at 1 month (Figure 2B), in 49 eyes (62.8%) at 3 months (Figure 2C), and in 53 eyes (67.9%) at 6 months postoperatively (Figure 2D), while there were no FAF signals in the macula (Figure 3, B–D) until 6 months postoperatively in 25 eyes (32.1%).

Fifty eyes (64.1%) had a continuous ELM line on the foveal OCT images, which corresponds to ELM recovery 1 month after surgery (Figure 2B), whereas in 42 eyes, the ELM line showed a defect (Figure 3B), which indicates that the ELM had not recovered. Continuous ELM lines on OCT images were seen in 67 eyes (85.9%) at 3 months (Figures 2C, 3C) and in 76 eyes (97.4%) at 6 months (Figures 2D, 3D) after surgery.

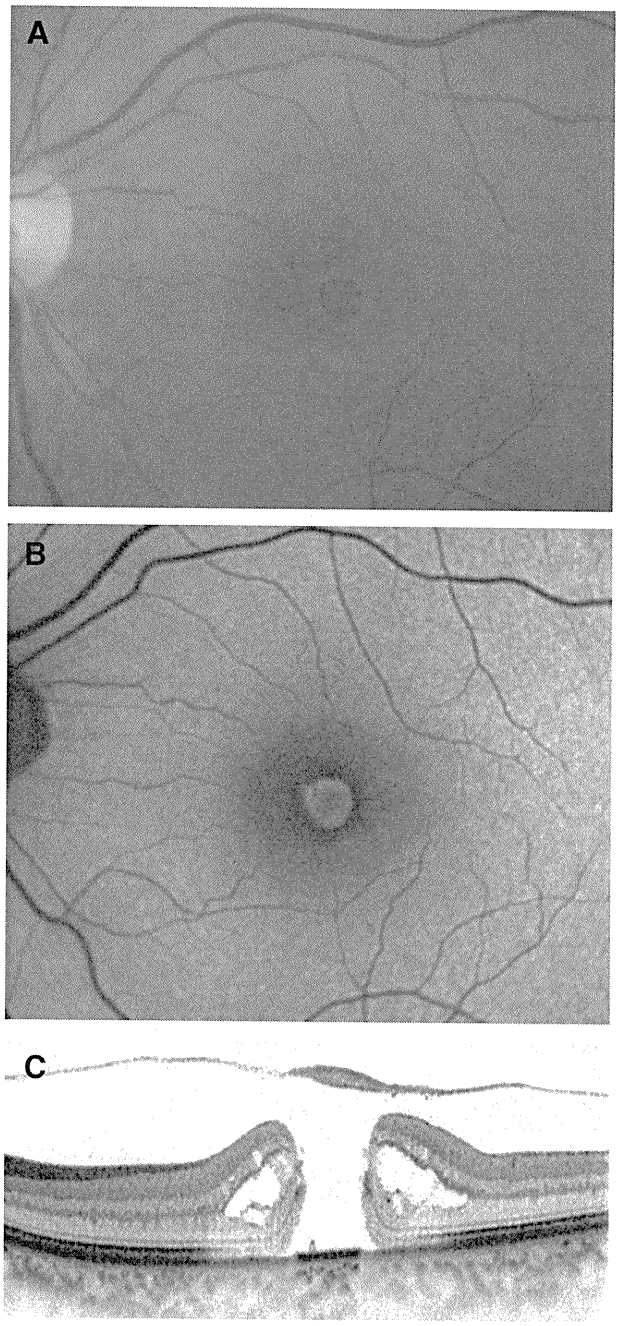

Fig. 1. Case 1. A 70-year-old man with a stage 3 MH in his left eye. **A.** The preoperative visual acuity was 20/50. The preoperative color photograph indicates MH with a surrounding fluid cuff. **B.** The FAF image taken preoperatively demonstrates increased FAF corresponding to the defect of the neurosensory retina. **C.** The optical coherence tomographic image taken preoperatively.

In contrast, only 6 of the 78 eyes (7.7%) had the continuous IS/OS line (Figures 2B, 3B) at 1 month postoperatively. The continuous IS/OS line recovery on OCT images was seen in 41 eyes (52.6%) at

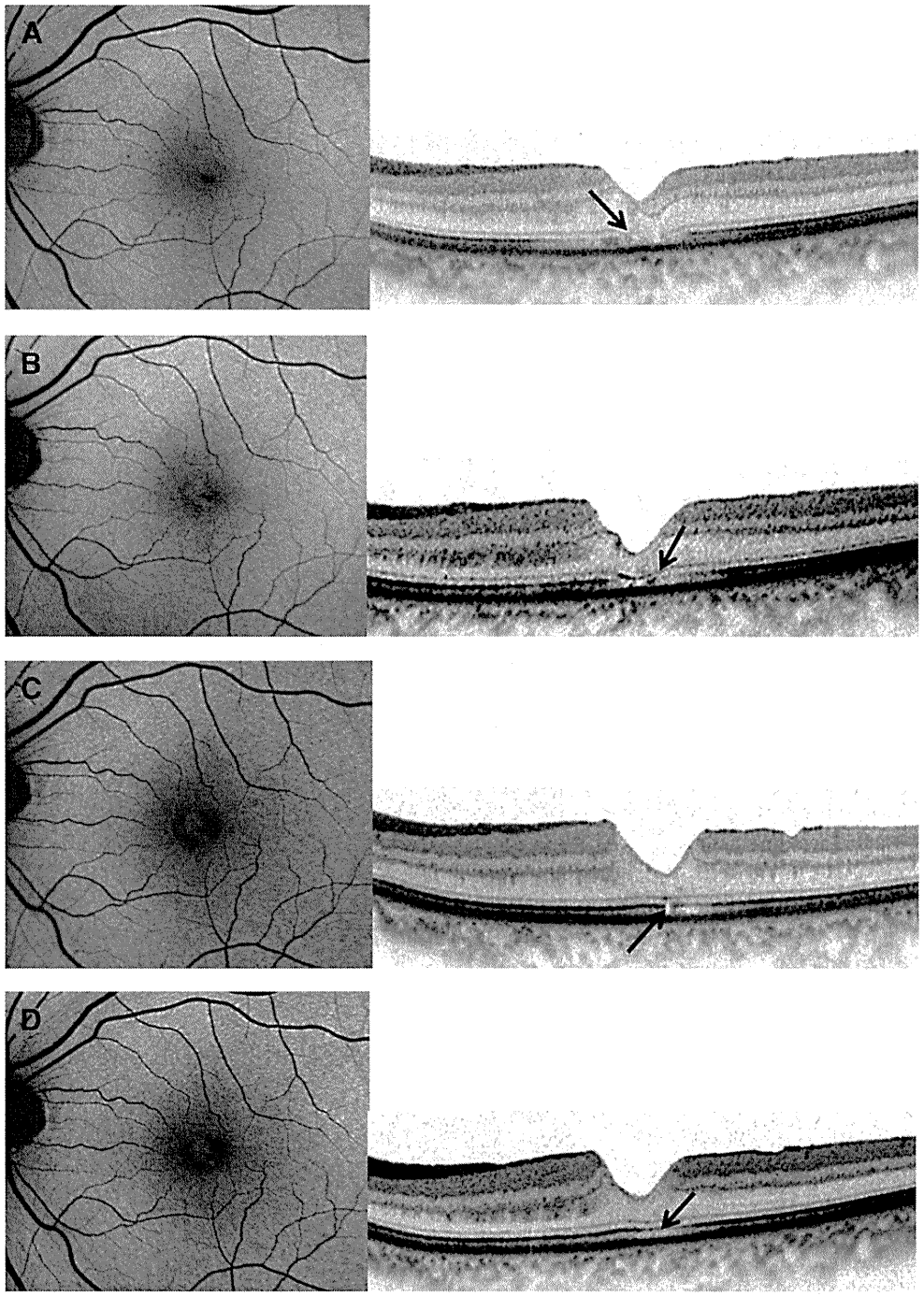

Fig. 2. The postoperative FAF images and OCT in Case 1. **A.** The FAF image (left) and OCT (right) taken 10 days postoperatively. The FAF demonstrates a decreased FAF signal at the closed macular area, and an outer foveal defect with disrupted ELM line and IS/OS line remains (arrow). **B.** FAF image taken 1 month postoperatively demonstrates a mild increased FAF signal at the closed MH (left). The OCT taken 1 month postoperatively shows a continuous ELM line (arrow), although an IS/OS line is disrupted (right), and the BCVA was increased to 20/22. **C.** FAF image taken 3 months postoperatively demonstrates the increased FAF signal at the closed MH (left). The OCT taken 3 months postoperatively shows a continuous ELM line and an IS/OS line with a minimal defect (right; arrow), and the BCVA was 20/20. **D.** FAF image taken 6 months postoperatively is almost the same as the FAF in the left panel. The OCT taken 6 months postoperatively shows a continuous ELM line and a continuous IS/OS line (right; arrow), and the BCVA was 20/20.

3 months (Figure 2C) and in 65 eyes (83.3%) at 6 months (Figure 2D) postoperatively.

In 25 patients whose macula continued showing hypoautofluorescence during observation 6 months after surgery (Figure 3), ELM line recovery was seen in only 8 eyes and IS/OS line recovery in only 1 eye 1 month after surgery. Eventually, in these cases of hypoautofluorescence in the macula, the recovery of ELM and IS/OS lines was seen in 20 eyes (80%) and 18 eyes (72%), respectively, 6 months postoperatively. It was obvious that, in cases of a hypoautofluorescent macula on FAF images, morphologic recovery of ELM and IS/OS lines was delayed, compared with the cases of hyperautofluorescent macula (Figure 3, B–D).

In all patients, the inner retinal layer, such as the inner nuclear layer, and the inner and outer plexiform layers, recovered with time. After 1 month to 3 months after the MH surgery, the structure of the inner retinal

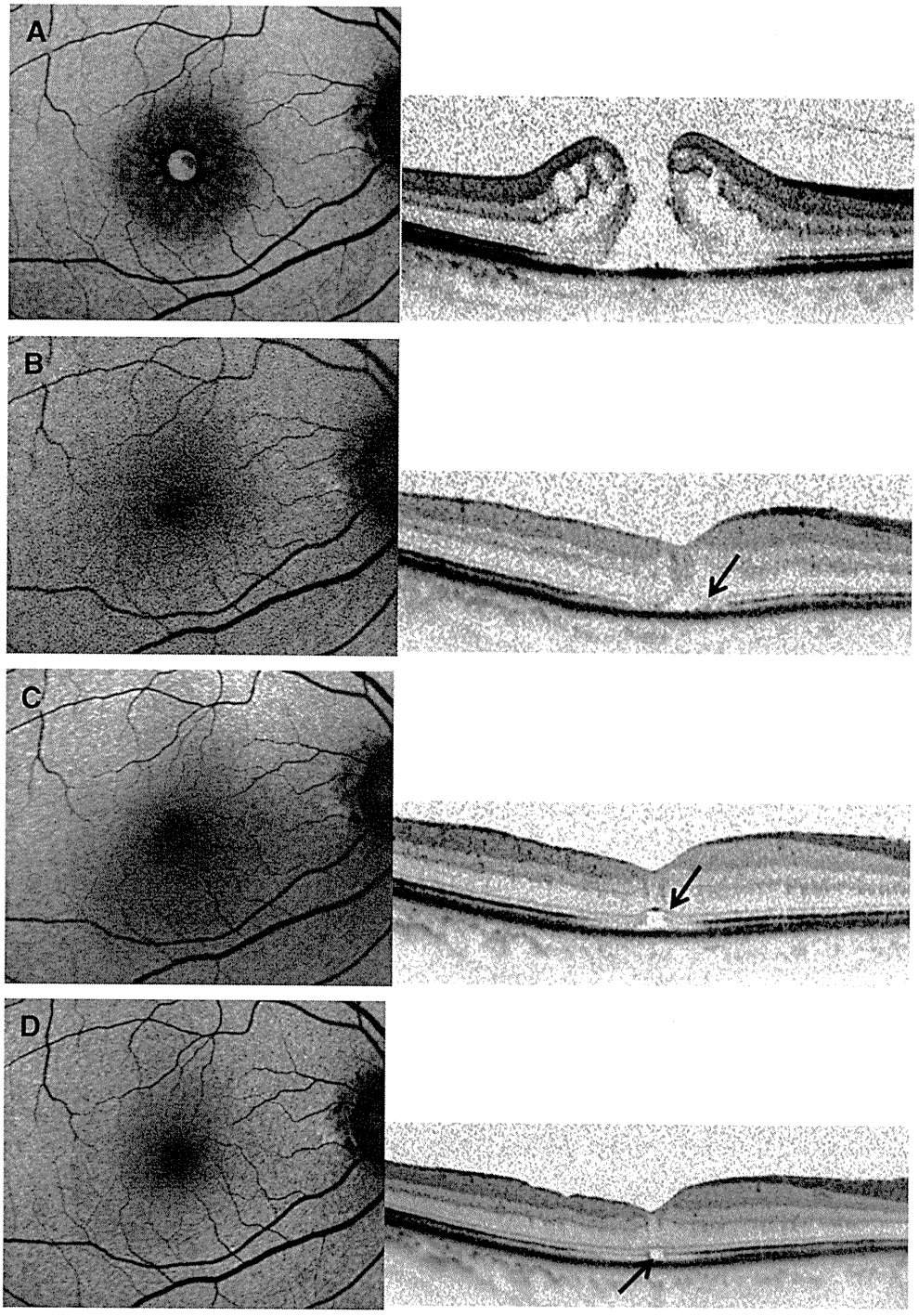

Fig. 3. Case 2. A 71-year-old woman with a stage 3 MH in her right eye. **A.** The preoperative BCVA was 20/50. The FAF image (left) taken preoperatively demonstrates increased FAF corresponding to the defect of the neurosensory retina (right). **B.** The FAF image taken 1 month postoperatively demonstrates hypofluorescence in the macula (left). The OCT taken 1 month postoperatively shows a disrupted ELM line (arrow) and a disrupted IS/OS line (right), and the BCVA remains 20/50. **C.** FAF image taken 3 months postoperatively demonstrates hypofluorescence in the macula (left). The OCT taken 3 months postoperatively shows a continuous ELM line (arrow) and foveal detachment with a disrupted IS/OS line (right). **D.** FAF image taken 6 months postoperatively still demonstrates hypofluorescence in the macula (left). The disruption of the IS/OS line (arrow) remains 6 months postoperatively (right). The BCVA was not improved.

layer appeared quite normal on the OCT images (Figures 2B, 3C).

Changes in the logMAR BCVA at 6 months postoperatively showed significant differences between the ELM recovery group and ELM nonrecovery group 1 month postoperatively (Student *t*-test, $P < 0.001$; Figure 4). Although, the features of the outer photoreceptor layer on the OCT images showed that the ELM lines recovered earlier than the IS/OS lines in the eyes of all patients, the IS/OS line recovery at 3 months postoperatively was significantly correlated with the ELM recovery at 1 month postoperatively ($P < 0.001$).

The appearance of increased FAF signals 1 month postoperatively was significantly associated with the ELM recovery at the fovea 1 month postoperatively

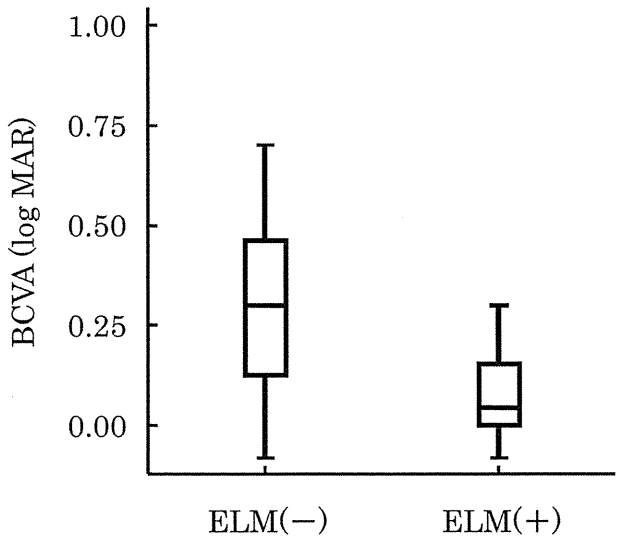

Fig. 4. Box plots showing BCVA 6 months after MH surgery in the group in which ELM recovery was not present 1 month after surgery (ELM−) and in the group with early ELM recovery 1 month after surgery (ELM+). The boxes show the median (line) and 25th and 75th percentiles. LogMAR, logarithm of the minimal angle of resolution.

(P = 0.001; Table 1). Moreover, good BCVA of 20/28 or better 6 months after the surgery was significantly associated with increased macular FAF 1 month postoperatively (P = 0.003), good preoperative visual acuity (P = 0.007), and IS/OS line recovery at the fovea 3 month postoperatively (P = 0.029; Table 2).

Discussion

Fundus autofluorescence imaging using a confocal scanning laser ophthalmoscope derives from the lipofuscin-laden RPE.[4,9] The autofluorescence is attenuated by the luteal pigment in the macula. Therefore, an autofluorescent spot in the macula is consistent with a loss of the foveal tissue, either partial (lamellar MH) or complete full-thickness MH.[4] Disappearance of FAF from the MH, as occurs after successful surgical repair,[3,4] suggests that, in our case, the RPE was again covered by the retinal and/or glial tissue, as demonstrated also by the OCT images. In our study, the completely closed MH after successful surgical treatment showed disappearance of autofluorescence 10 days postoperatively, similar to the normal fundus. In the eyes of almost half of the total number of patients (46.2%), closed macular areas again showed mildly increased FAF signals 1 month after surgery. Whereas the appearance of increased FAF signals 1 month postoperatively was significantly associated with early ELM recovery at the fovea 1 month postoperatively, postoperative good BCVA of 20/28 or better 6 months after MH closure was significantly associated with increased FAF, preoperative BCVA, and IS/OS recovery at 3 months postoperatively. Also, these results indicate that this increased FAF signal may predict a good visual prognosis after MH surgery. Early ELM recovery at the fovea 1 month postoperatively was significantly associated with IS/OS recovery 3 months postoperatively. The reason why the closed MH area shows an increased FAF signal is however unclear.

Generally, in normal eyes, macular pigment, which is composed of lutein and zeaxanthin, is important for the maintenance of macular health through its absorptive and/or antioxidant properties.[15–18] These compounds are especially dense in the axons of cone photoreceptors at the fovea, although cells in the inner nuclear layer and the inner and outer plexiform layers also contain these compounds.[15–18] After successful MH closure, the structure of the retinal layer in the macula may not recover completely. Hangai et al[19] reported that centrifugal enlargement of tiny interruptions in the ELM occurs in an MH if the Muller cell cone is dragged away. Their report proved that there is less of a defect in the tissue in MH but rather centrifugal displacement of the photoreceptors occurs. Because

Table 1. Multiple Logistic Regression Model of Variables Associated with Increased FAF 1 Month After MH Closure

	Odds Ratio	95% CI	P
Age	0.971	0.906–1.041	0.405
ELM line recovery*	8.230	2.441–27.750	0.001
IS/OS line recovery*	1.588	0.246–10.259	0.627
Preoperative BCVA	0.514	0.034–7.758	0.631
Stage	1.221	0.634–2.354	0.550

CI, confidence interval.
*1 month after MH surgery.

Table 2. Multiple Logistic Regression Model of Variables Associated with Postoperative Good Visual Acuity 6 Months After MH Closure

	Odds Ratio	95% CI	P
Age	0.976	0.898–1.060	0.563
Increased FAF*	7.376	1.986–27.397	0.003
Preoperative BCVA	192.398	4.313–8583.242	0.007
IS/OS line recovery†	4.181	1.154–15.153	0.029
Preoperative historical duration	0.725	0.521–1.008	0.056
Stage	0.772	0.348–1.713	0.525
ILM staining	1.934	0.563–6.640	0.295

*1 months after MH surgery.
†3 months after MH surgery.

ELM is a part of Muller cells, early ELM recovery might indicate early recovery of the retinal morphologic structure, including inner retinal layers. The ELM lines recovered earlier than the IS/OS lines in the eyes of all patients, and the IS/OS line recovery at 3 months postoperatively was significantly correlated with the ELM recovery at 1 month postoperatively. Moreover, the continuous IS/OS line recovery at the fovea 3 months postoperatively is significantly associated with a good visual prognosis 6 months postoperatively. Briefly, the presence of a normal IS/OS line may indicate morphologic and functional recovery of the photoreceptors.[17] In our study, the increased FAF signal 1 month postoperatively, which was almost absent 10 days postoperatively, was significantly associated with early ELM recovery. The factors influencing this increase in the eyes that had early ELM recovery resulting in a good visual prognosis may include the morphologic changes of the inner retinal layers, for example, lateral displacement of the inner retinal layers with time (Figure 2). It is hypothesized that if displacement of the macular pigment–containing inner retinal layers exists at the fovea soon after the surgery and if the RPE function is normal at the macular area, the hyperautofluorescence may be concealed by the macular pigment. Later, the inner retinal layers move to the normal position with time and the hyperautofluorescence can be seen through the damaged macula with decreasing pigment concentration after the surgery. In this study, 46.2% eyes showed hyperautofluorescence at the macular area 1 month postoperatively. This result indicates that, in those eyes, hyperautofluorescence was caused by both the decreased macular pigment and the RPE that had normal metabolic function.

In contrast, late ELM recovery indicates insufficient recovery of the retinal structure leading to late IS/OS recovery resulting in photoreceptor dysfunction at the fovea after MH surgery. In the human RPE, lipofuscin accumulates as a by-product of phagocytosis of the photoreceptor outer segments. Fundus autofluorescence in the RPE depends on the outer segment renewal and is potentially affected by a balance between accumulation and clearance. So, the late IS/OS line recovery might be the reason for decreased FAF signals at closed macula after surgery; in other words, the disappearance of FAF as a surrogate marker for monitoring the functional recovery of the photoreceptors and the restoration of RPE–photoreceptor interactions in repaired MH, the complete disappearance of increased FAF and a loss of pigment or RPE death, respectively.

Another possible concern regarding the disappearance of FAF as a surrogate speculated that the restoration of hypoautofluorescence in the fovea after MH surgery could not be achieved without recovery of the inner retinal layer. Simply extending neurosensory retinal or glial tissues over the bare RPE after MH surgery would not result in complete disappearance of FAF. Improved visual acuity of patients with repaired MHs obviously implies that the photoreceptor function is recovered, both morphologically and functionally. The interpretation of FAF in repaired MH could be complicated because it might also be influenced by other cells and tissues in the fovea as a result of their minor contributions to the macular pigment.

In this study, the historical duration of MH was not significantly associated with visual prognosis but tended to be correlated with good visual prognosis ($P = 0.056$; Table 2) This shows that, in chronic MH, once the bare RPE is surgically covered with neurosensory retinal tissue, normal interactions between the RPE and the photoreceptors may be slightly difficult.

In conclusion, increased FAF early after MH surgery is an important indicator of ELM recovery leading to the early recovery of photoreceptors, predicting a good postoperative visual prognosis. This increased FAF signal may be induced by normal metabolic activity of the RPE cells along with normal photoreceptor recovery. Further careful investigation and long-term follow-up of these patients are required to better understand the usefulness of FAF after MH surgery.

Key words: fundus autofluorescence, external limiting membrane, idiopathic full-thickness macular hole, spectral-domain optical coherence tomography.

References

1. Gass JDM. Reappraisal of biomicroscopic classification of stages of development of a macular hole. Am J Ophthalmol 1995;119:752–759.
2. Milani P, Seidenari P, Carmassi L, Bottoni F. Spontaneous resolution of a full thickness idiopathic macular hole: fundus autofluorescence and OCT imaging. Graefes Arch Clin Exp Ophthalmol 2007;245:1229–1231.
3. Ciardella AP, Lee GC, Langton K, et al. Autofluorescence as a novel approach to diagnosing macular holes. Am J Ophthalmol 2004;137:956–959.
4. von Rückmann A, Fitzke FW, Gregor ZJ, Fundus autofluorescence in patients with macular holes imaged with a laser scanning ophthalmoscope. Br J Ophthalmol 1998;82:346–351.
5. Spaide RF. Autofluorescence from the outer retina and subretinal space: hypothesis and review. Retina 2008;28:5–35.

6. Spaide RF. Fundus autofluorescence and age-related macular degeneration. Ophthalmology 2003;110:392–399.
7. Chung JE, Spaide RF. Fundus autofluorescence and vitelliform macular dystrophy. Arch Ophthalmol 2004;122:1078–1079.
8. Schmitz-Valckenberg S, Holz FG, Bird AC, Spaide RF. Fundus autofluorescence imaging: review and perspectives. Retina 2008;28:385–409.
9. Delori FC, Dorey CK, Staurenghi G, et al. In vivo fluorescence of the ocular fundus exhibits retinal pigment epithelium lipofuscin characteristics. Invest Ophthalmol Vis Sci 1995;36:718–729.
10. Snodderly DM, Auran JD, Delori FC. The macular pigment. II. Spatial distribution in primate retinas. Invest Ophthalmol Vis Sci 1984;25:674–685.
11. Chung H, Shin CJ, Kim JG, et al. Correlation of microperimetry with fundus autofluorescence and spectral-domain optical coherence tomography in repaired macular holes. Am J Ophthalmol 2011;151:128–136.
12. Inoue M, Watanabe Y, Arakawa A, et al. Spectral-domain optical coherence tomography images of inner/outer segment junctions and macular hole surgery outcomes. Graefes Arch Clin Exp Ophthalmol 2009;247:325–330.
13. Sano M, Shimoda U, Hashimoto H, Kishi S. Restored photoreceptor outer segment and visual recovery after macular hole closure. Am J Ophthalmol 2009;147:313–318.
14. Enaida H, Hisatomi T, Hata Y, et al. Brilliant blue G selectively stains the internal limiting membrane/brilliant blue G-assisted membrane peeling. Retina 2006;26:631–636.
15. Neelam K, O'Gorman N, Nolan J, et al. Macular pigment levels following successful macular hole surgery. Br J Ophthalmol 2005;89:1105–1108.
16. Beatty S, Boulton ME, Henson DB, et al. Macular pigment and age related macular degeneration. Br J Ophthalmol 1999;83:867–877.
17. Davies NP, Morland AB. Macular pigments: their characteristics and putative role [review]. Prog Retin Eye Res 2004;23:533–559.
18. Schütt F, Davies S, Kopitz J, et al. Photodamage to human RPE cells by A2-E, a retinoid component of lipofuscin. Invest Ophthalmol Vis Sci 2000;41:2303–2308.
19. Hangai M, Ojima Y, Gotoh N, et al. Three-dimensional imaging of macular holes with high-speed optical coherence tomography. Ophthalmology 2007;114:763–773.

Current Eye Research, 36(11), 1037–1046, 2011

ISSN: 0271-3683 print/ 1460-2202 online
DOI: 10.3109/02713683.2011.594201

informa
healthcare

ORIGINAL ARTICLE

Deleterious Role of Anti-high Mobility Group Box 1 Monoclonal Antibody in Retinal Ischemia-reperfusion Injury

Shenyang Yang[1,3], Kazuyuki Hirooka[1], Ye Liu[1,5], Tomoyoshi Fujita[1], Kouki Fukuda[1], Takehiro Nakamutra[2], Toshifumi Itano[2], Jiyong Zhang[4], Masahiro Nishibori[4], and Fumio Shiraga[1]

[1]Department of Ophthalmology, Kagawa University Faculty of Medicine, Kagawa, Japan, [2]Department of Neurobiology, Kagawa University Faculty of Medicine, Kagawa, Japan, [3]Department of Ophthalmology, Shengjing Affiliated Hospital, China Medical University, Shenyang, China, [4]Department of Pharmacology, Okayama University Graduate School of Medicine, Density and Pharmaceutical Sciences, Okayama, Japan, and [5]Department of Ophthalmology, The Fourth Affiliated Hospital, China Medical University, Shenyang, China

ABSTRACT

Purpose: To investigate the effect of anti-high mobility group box 1 (HMGB1) monoclonal antibody (mAb) against ischemia-reperfusion injury in the rat retina.

Materials and Methods: Retinal ischemia was induced by increasing and then maintaining intraocular pressure at 130 mmHg for 45 min. An intraperitoneal injection of anti-HMGB1 mAb was administered 30 min before ischemia. Retinal damage was evaluated at 7 days after the ischemia. Immunohistochemistry and image analysis were used to measure changes in the levels of reactive oxygen species (ROS) and the localization of anti-HMGB1 mAb. Dark-adapted full-field electroretinography (ERG) was also performed.

Results: Pretreatment with anti-HMGB1 mAb significantly enhanced the ischemic injury of the retina. HMGB1 expression increased at 6–12 h after ischemia in the retina. After the ischemia, production of ROS was detected in retinal cells. However, pretreatment with anti-HMGB1 mAb increased the production of ROS. On the seventh postoperative day, the amplitudes of both the ERG a- and b-waves were significantly higher in the vehicle group than in the groups pretreated with anti-HMGB1 mAb.

Conclusions: The current *in vivo* model of retinal injury demonstrated that anti-HMGB1 mAb plays a large deleterious role in ischemia-reperfusion injury. In order to develop neuroprotective therapeutic strategies for acute retinal ischemic disorders, further studies on anti-HMGB1 mAb function are needed.

Keywords: Anti-HMGB1 mAb, Retinal ischemia, Reactive oxygen species, Electroretinogram, Retinal thickness

INTRODUCTION

Ischemic injury to the retina is a major cause of visual loss and morbidity. As these morbidities are difficult to treat, research into various potential treatments is currently ongoing.[1–5] Ischemia-reperfusion injury involves many signaling mechanisms that ultimately result in necrotic and apoptotic cell death.[6] Delayed neuronal cell death in the brain and retina secondary to transient ischemic injury occurs, in part, by apoptosis.[7,8] During or after ischemia, reactive oxygen species (ROS) can be produced in large quantities and act as cytotoxic metabolites.[9] ROS can provoke cell death by reacting with cell components that lead to necrosis, or by activating specific targets that trigger apoptosis.

High-mobility group box-1 (HMGB1) protein was originally described 30 years ago as a nonhistone DNA-binding protein with high-electrophoretic mobility.[10] HMGB1 is a nuclear protein involved in nucleosome stabilization and gene transcription.[11] It is known that these functions are essential for survival, as HMGB1-deficient mice have been shown to die of hypoglycemia within 24 h of birth.[12] HMGB1 is

Received 19 November 2010; accepted 31 May 2011

Correspondence: Kazuyuki Hirooka, MD, PhD, Department of Ophthalmology, Kagawa University Faculty of Medicine, 1750-1 Ikenobe, Miki, Kagawa 761-0793 Japan. Tel: +81 87 891 2211. Fax: +81 87 891 2212. E-mail: kazuyk@med.kagawa-u.ac.jp

found in almost all eukaryotic cells, and its presence has been confirmed in the rodent retina.[13] HMGB1 has also been implicated in the mechanism of ischemic brain damage.[14–20] In a stroke model, short hairpin (sh) RNA-mediated HMGB1 down-regulation in the brain reduces the severity of lesions.[15] Intravenous injection of the anti-HMGB1 monoclonal antibody (mAb) causes a dramatic reduction in the infarct size in the stroke model.[17]

The purpose of the present study was to investigate the role of anti-HMGB1 and its specific expression in retinal ischemia-reperfusion injury.

MATERIAL AND METHODS

Animals

Male Sprague-Dawley rats weighing 200–250 g were obtained from Charles River Japan (Yokohama, Japan). Rats were permitted free access to standard rat food (Oriental Yeast Co., Ltd., Tokyo, Japan) and tap water. Animal care and all experiments were conducted in accordance with the approved standard guidelines for animal experimentation of the Kagawa University Faculty of Medicine, and adhered to the ARVO Statement for the Use of Animals in Ophthalmic and Vision Research. Anti-HMGB mAb or IgG2a was injected by three different methods. Intraperitoneal injection of anti-HMGB1 monoclonal antibody (mAb) (200 μg)[17] or class-matched control mAb (IgG2a) (200 μg) against *Keyhole Limpet* hemocyanin was administered 30 min before ischemia. Anti-HMGB mAb (200 μg) or IgG2a (200 μg) was administered intravenously immediately and 6 h after reperfusion. The pupil was dilated with topical phenylephrine hydrochloride and tropicamide; anti-HMGB mAb (20 μg) or IgG2a (20 μg) was injected into the vitreous space 30 min before ischemia.

Ischemia

Rats were anesthetized by an intraperitoneal injection of 50 mg/kg pentobarbital sodium (Abbott, Abbott Park, IL) followed by a topical administration of 0.4% oxybuprocaine hydrochloride. The anterior chamber of the right eye was cannulated with a 27-gauge infusion needle connected to a reservoir containing normal saline. The intraocular pressure (IOP) was raised to 130 mmHg for 45 min by elevating the saline reservoir. Only the right eye of each rat was subjected to ischemia. Retinal ischemia was indicated by whitening of the iris and fundus. The left eyes served as the sham-treated controls, with these eyes undergoing a similar procedure that did not include elevation of the saline bag, thus maintaining normal ocular tension. Rectal and tympanic temperatures were maintained during the operation at approximately 37°C via the use of a feedback-controlled heating pad (BRC, Nagoya, Japan). After restoration of blood flow, temperature was maintained continuously at 37°C.

HISTOLOGICAL EXAMINATION

For histological examination, rats were anesthetized by intraperitoneal injection of pentobarbital sodium (50 mg/kg) 7 days after ischemia. Eyes were enucleated and stored in a 4% paraformaldehyde solution for 24 h at room temperature. The retinas were removed and embedded in paraffin, and thin sections (5-μm thickness) were cut using a microtome. Each retina was mounted on a silane-coated glass slide and then stained with hematoxylin and eosin (HE).

Morphometric analysis was performed to quantify ischemic injury. These sections were selected randomly in each eye. Light microscopic examination was performed by a person with no prior knowledge of the treatments. A microscopic image of sections obtained within 0.5–1 mm of the optic disc was scanned. For each computer image, the number of cells in the ganglion cell layer (GCL) was counted. The thicknesses of the inner plexiform layer (IPL), inner nuclear layer (INL), outer nuclear layer (ONL), and outer plexiform layer (OPL) for the entire frame were measured. The number of cells in the GCL was normalized as linear cell density (cells per millimeter). Thicknesses of the IPL, INL, ONL, and OPL were obtained by calculating the mean value of seven measurements in each eye. Similarly, the linear cell density in the GCL was also determined by calculating the mean value of seven measurements. For each animal, the right eye parameter was normalized to that of the intact left eye and shown as a percentage.

ELECTRORETINOGRAMS (ERGS)

ERG responses were measured after overnight dark adaptation (at least 6 h) using a recording device (Mayo Corporation, Aichi, Japan) 7 days after ischemia. Rats were anesthetized by an intraperitoneal injection of 50 mg/kg pentobarbital sodium. Pupils were dilated with 0.5% tropicamide and 0.5% phenylephrine hydrochloride eye drops (Santen Pharmaceuticals, Osaka, Japan). All procedures were performed in dim red light, with all rats kept warm during the procedure. The LED corneal electrode was set vertical to the cornea center. A reference electrode was set subcutaneously on the forehead and the ground connection was set on the base of the tail. An LED stimulator LS-W controlled the stimulus duration and intensity during the 11-step intensity series, which ranged from 0.0003–30 cds/m^2. The ERG response was amplified using an AC amplifier ML135 (Bio Amplifier, AD Instruments, NSW, Australia) with a bandwidth of 0.3–500 Hz and amplification of 2,000 times. The ischemic damage to the retina was

evaluated as the percentage of the a- and b-wave amplitudes of the ischemic right eyes as compared to the non-ischemic left eyes.

IMMUNOHISTOCHEMISTRY

Eyes were enucleated at 6, 12 or 24 h after 45 min of ischemia. Eyes were then fixed in 4% paraformaldehyde in the PBS and embedded in paraffin. Retinal sections (5 μm) were rinsed in 100% ethanol twice for 5 min each, followed by a separate 95% ethanol and 90% ethanol rinse for 3 min each. The sections were then washed using PBS, pH 7.4, three times for 10 min each and treated with 0.3% Triton X-100 in PBS, pH 7.4, for 1 h. After further washing three times for 10 min each with PBS, pH 7.4, sections were then blocked in 3% normal horse serum and 1% bovine serum albumin (BSA) in PBS for 1 h in order to reduce nonspecific labeling. Sections were incubated overnight at 4°C in PBS with either 2.0 mg/mL of monoclonal antibody against HMGB1[17] which served as the primary antibody. After washing in PBS for 50 min, sections were then immersed in the second antibody conjugated to horseradish peroxidase for 1 h at room temperature. Images were acquired using 40× objective lenses (DXM 1200; Nikon, Tokyo, Japan). Adobe PhotoShop v. 5.0 was used to adjust the brightness and contrast of the images.

FLUORESCENT LABELING OF ROS

To investigate the production of ROS, we intraperitoneally injected 5 mg/kg dihydroethidium (DHE; Sigma-Aldrich, St. Louis, MO) in 5% dimethyl sulfoxide (DMSO) in PBS 15 min before ischemia. A 0.3-mL aliquot of distilled water, 200 μg anti-HMGB1 mAb, or 200 μg IgG2a was administered intraperitoneally 30 min before ischemia. Eyes were enucleated 15 min after ischemia and then embedded in OCT compound (Sakura Finetek, Torrance, CA), after which cryosections (20 μm) were prepared. Sections were examined with a microscope (Radiance 2100/Rainbow, Carl Zeiss, München, Germany) using a laser set (excitation laser 514 nm; emission laser >580 nm).

Statistical Analysis

Fluorescence was quantified by automated image analysis with Image-Pro Plus software (version 4.0, Media Cybernetics, The Imaging Expert, Bethesda, MD). For each section, mean fluorescence was calculated from five separate high-power fields per eye. A threshold was set to define positive labeling.

All data are presented as the mean ± SD. Data were analyzed using an independent Student's *t*-test and ANOVA followed by Tukey-Kramer post-hoc testing corrected for multiple comparisons. Statistical analysis was performed using SPSS for Windows (SPSS Inc, Chicago, IL). A p value of < 0.05 was considered statistically significant.

RESULTS

Histologic Changes in the Retina after Ischemia with Anti-HMGB1

Figure 1A shows a normal retina. Light microscopic photographs were taken 7 days after ischemia and treatment with IgG2a (Figure 1B) or anti-HMGB1 (Figure 1C). In animals pretreated with IgG2a, the GCL cell number was reduced to 73.9 ± 16.2% of the control; the IPL thickness was reduced to 67.7 ± 14.6% of the control; the INL thickness was reduced to 82.8 ± 13.5% of the control; the OPL thickness was reduced to 88.6 ± 30.8% of the control; and the ONL thickness was reduced to 88.1 ± 13.0% of the control ($n=7$; Figure 1D). In animals pretreated with anti-HMGB1 mAb, the GCL cell numbers were 67.7 ± 16.8% of the control ($p=0.50$); the IPL thickness was 51.6 ± 12.3% of the control ($p=0.02$); the INL thickness was 69.0 ± 6.8% of the control ($p=0.03$); the OPL thickness was 51.9 ± 10.8% of the control ($p=0.01$); and the ONL thickness was 72.4 ± 13.7% of the control ($p=0.049$) ($n=7$; Figure 1D).

Treatment with intravenous injection of IgG2a or anti-HMGB1 mAb twice (immediately and 6 h after reperfusion) reduced the retinal thickness dramatically (n = 4, each group) (Figure 2).

Treatment with local administration of IgG2a or anti-HMGB1 mAb 30 min before ischemia was similar to the results with intraperitoneal injection of anti-HMGB1 mAb ($n=4$, each group) (Figure 3).

EFFECT OF ANTI-HMGB1 ON NORMAL RETINA

Animals were killed at 7 days after the intraperitoneal injection of anti-HMGB1 mAb or IgG2a. Treatment with anti-HMGB1 did not affect the retinal thickness in normal rat (Figure 4) ($n=4$, each group).

EFFECT OF ANTI-HMGB1 ON RETINAL FUNCTION

Scotopic ERG was recorded to evaluate anti-HMGB1 mAb effects on retinal function. A representative example of function is seen in Figure 5A. Mean amplitudes of the a- and b-wave are shown in Figure 5B. We observed a statistically significant difference between the three groups ($n=5$, each group).

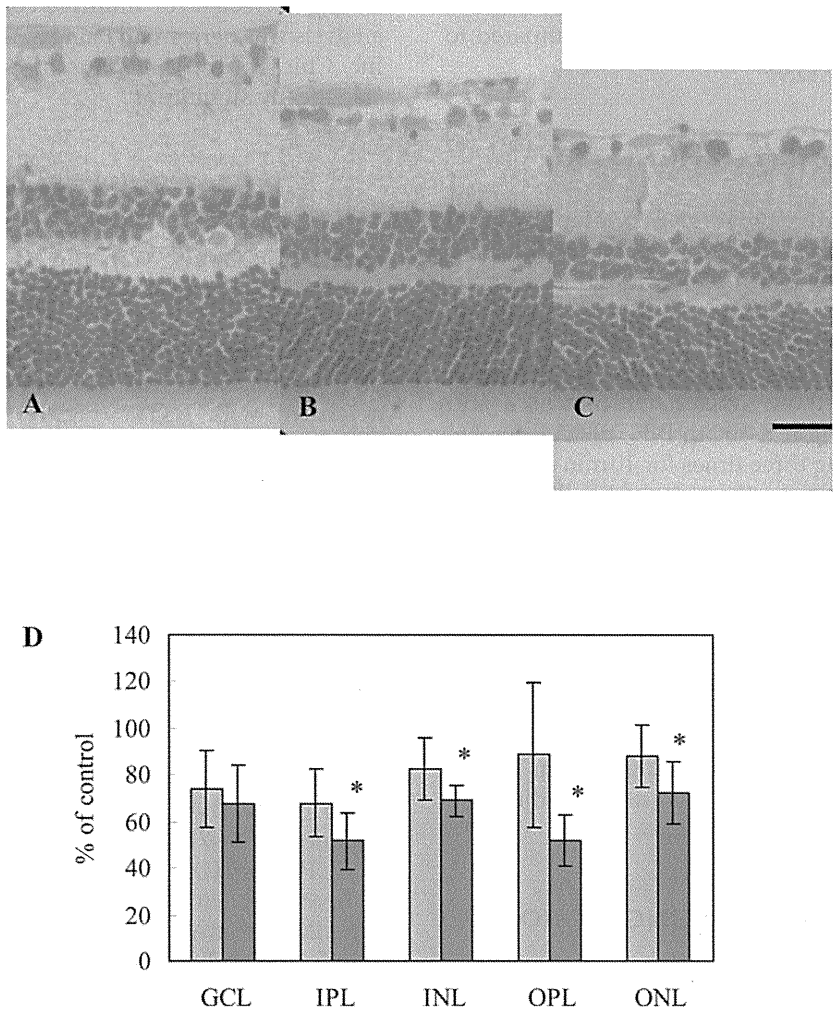

FIGURE 1 Light micrographs of a cross-section through normal rat retina (A) and at 7 days after ischemia when treated with control class-matched mAb (anti-*Keyhole Limpet* hemocyanin mAb, IgG2a) (B) or anti-HMGB1 mAb (C). Percentages indicate change relative to control values for the number of GCL cells and for the IPL, INL, ONL, and OPL thicknesses 7 days after ischemia when treated with IgG2a (▒) or anti-HMGB1 (■). Results are expressed as the mean ± SD (*$p < 0.05$). Scale bar = 20 μm.

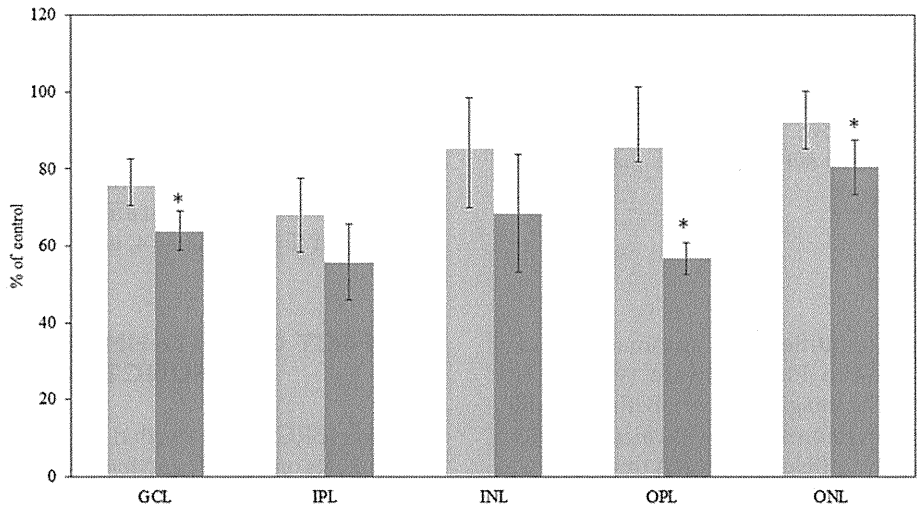

FIGURE 2 Percentages indicate change relative to control values for the number of RGC cells and for IPL, INL, ONL, and OPL thickness 7 days after ischemia when treated with intravenous injections of IgG2a (▒) or anti-HMGB1 (■). Results are expressed as the mean ± SD (*$p < 0.05$).